

## Development of Gamma Ray Monitor Using CdZnTe Semiconductor Detector

A. H. D. Rasolonjatovo, T. Shiomi, T. Nakamura, H. Nishizawa<sup>1</sup>,  
Y. Tsudaka<sup>1</sup>, H. Fujiwara<sup>1</sup>, H. Araki<sup>1</sup>, and K. Matsuo<sup>1</sup>

*Department of Quantum Science and Energy Engineering, Tohoku University  
Aza-aoba, Amaraki, Aoba-ku, Sendai, Miyagi 980-8578, JAPAN*

<sup>1</sup>*Mitsubishi Electric Corporation*

*8-1-1, Tsukaguchi-Honmachi, Amagasaki, Hyogo 661, JAPAN*

### Abstract

In this study, we aimed to develop a new X-ray and gamma ray monitor using the CdZnTe semiconductor detector, which have high sensitivity at room temperature. The pulse height spectra and the detection efficiencies of 10x10 mm<sup>2</sup> by 2 mm thick CdZnTe detector were measured in the energy range of 10 keV to 1.8 MeV by using monoenergetic X-ray and gamma ray sources. The measured results showed very good agreement with the results calculated using the EGS4 Monte Carlo code taking into account the charge collection efficiency in the detector. By using two CZT detectors of 10x10x2 mm<sup>3</sup> and 3x3x2 mm<sup>3</sup> coupled with a filter, the weighted sum of a few energy channels with different cut-off energies was finally found out to realize a flat energy response to equivalent dose (counts per mSv) within  $\pm 30\%$  or  $\pm 10\%$  deviation.

## 1 Introduction

In recent years the CdZnTe (CZT) semiconductor detector is preferred for X-ray and low energy gamma ray detection in many situations, because of its high efficiency, low bias voltage, good energy resolution and its capability of operation at room and higher temperatures[1, 2, 3]. The CZT detector has a great advantage to have the high density ( $\rho = 5.86 \text{ g}\cdot\text{cm}^{-3}$ ) and the high atomic number ( $Z=48$  for Cd, 30 for Zn and 52 for Te) compared with Si ( $\rho=2.4 \text{ g}\cdot\text{cm}^{-3}$ ,  $Z=14$ ) and Ge ( $\rho=5.36 \text{ g}\cdot\text{cm}^{-3}$ ,  $Z=32$ ) semiconductor detectors. Nowadays a larger crystal size of CZT becomes available and the CZT detector can be used for higher energy gamma ray detection. In this study, we aimed to develop a new gamma ray monitor using a Cd<sub>0.5</sub>Zn<sub>0.5</sub>Te semiconductor detector. The present gamma ray monitor, therefore, possesses higher sensitivity than the commercially available Si semiconductor gamma ray monitor and at the same time has a flat energy response to dose-equivalent in the wide photon energy region from 10 keV to 7 MeV. This gamma ray monitor could be used to operate at higher temperature such as in the power reactor core.

## 2 Materials and Methods

As a gamma ray sensor, a Cd<sub>0.5</sub>Zn<sub>0.5</sub>Te detector having 10 mm x 10 mm size by 2 mm thickness (fabricated by eV Product, USA) was used. Table 1 shows the physical characteristics of the CZT detector used in this study. The detector was directly coupled to the low noise preamplifier (Model 850, fabricated by Clear-Pulse Co. Ltd, Japan). The bias voltage of +24 V was supplied to the detector from the regulated power supply (PR 36-1.2 A fabricated by Kenwood, Japan). The preamplifier was connected to a linear amplifier ORTEC 571 with a 2  $\mu\text{s}$  shaping time. The detector and the preamplifier were covered with an Al foil of 0.015 mm thickness to decrease the electromagnetic noise.

In order to get the energy response of the CZT detector, the measurements were done using the mono-energetic X-ray beam sources from 10 to 40 keV and the radioactive photon sources of  $^{241}\text{Am}$ ,  $^{57}\text{Co}$ ,  $^{137}\text{Cs}$ ,  $^{60}\text{Co}$  and  $^{88}\text{Y}$  having photon energies of 59.54 keV to 1836 keV.

The experiments using X-ray beam sources were performed at a beam line of the Photon Factory of High Energy Accelerator Research Organization (KEK), Tsukuba, Japan. Because a direct photon beam intensity from the beam line of synchrotron radiation is too high, a beam scattered at  $90^\circ$  was used. In order to investigate the variation of the energy response with the filters, we also measured the pulse height distributions of the CZT detector covered with Al, Cu, Cd and Pb filters of various thicknesses.

The measurements using point sources were carried out at the Hot Laboratory of the Cyclotron and Radioisotope Center (CYRIC), Tohoku University, Japan. The point sources of about 2 mm diameter are encapsulated within thin vinyl cover. The source was placed at 10 cm from the detector surface. The fraction of backscattered photons was about 2%. In order to get the angular dependence of the detection efficiency, the CZT detector was rotated to the source-to-detector axis in the directions of 0 to  $90^\circ$ . The  $^{137}\text{Cs}$  source was covered with a 1.5 mm thick Al foil to absorb the 661.7 keV conversion electrons from the electron capture reaction and the  $\beta$  rays of 511 keV. The  $^{60}\text{Co}$  was also covered with a 1 mm thick Al foil to absorb the  $\beta$  rays of 318 keV.

### 3 Calculations

The pulse height spectra of the detector were also calculated using the electron-photon cascade Monte Carlo code EGS4[4] taking into account the carrier trapping effect[5]. The charge collection depends on the drift distance of the hole and the electron, which vary with the depth of interaction in the detector.

For the CZT, the product of the mobility  $\mu$  and lifetime  $\tau$ , ( $\mu\tau$ ), is very low, especially for holes and then most of the holes are trapped before reaching the cathode. The mean free path is given by

$$\lambda = \mu\tau F = \mu\tau \frac{V}{d} \quad (1)$$

where  $F$  is the electric field,  $d$  is the thickness of the detector and  $V$  is the applied voltage.

In the present case, we calculated the deposited energy  $E$  in the CZT detector for the geometry that a plane parallel photon beam is incident normal to the detector surface using the EGS4-PRESTA code[4], and taking into account the carrier trapping effect. According to the work by Nishizawa et al.[5], three cases were considered: energy absorption only, constant drifting distance of the carrier and exponential distribution of the drifting distance of the carrier.

For the first case where energy absorption only is considered, the induced charges are independent to the interaction depth, then

$$Q(x) = Q_0 = \frac{E}{\varepsilon} e \quad (2)$$

$\varepsilon$  is the energy needed to create an electron-hole pair and is equal to 4.43 eV[6],  $E$  is the deposited energy and  $e$  is the charge of the electron ( $e = 1.6 \times 10^{-19}$  C).

For the second case, the induced charges can be written as the first-order approximation of the Fetch's equation[7] as follows[5]

$$\begin{aligned} \text{If } \lambda_e > d - x \text{ and } \lambda_h > x &\longrightarrow Q(x) = \frac{E}{\varepsilon} e, \\ \text{If } \lambda_e > d - x \text{ and } \lambda_h < x &\longrightarrow Q(x) = \frac{E}{\varepsilon} e \left[ \frac{d - x}{d} + \frac{\lambda_h}{d} \right], \\ \text{If } \lambda_e < d - x \text{ and } \lambda_h < x &\longrightarrow Q(x) = \frac{E}{\varepsilon} e \left[ \frac{\lambda_e}{d} + \frac{\lambda_h}{d} \right], \end{aligned}$$

$$\text{If } \lambda_e < d - x \text{ and } \lambda_h > x \longrightarrow Q(x) = \frac{E}{\varepsilon} e \left[ \frac{\lambda_e}{d} + \frac{x}{d} \right], \quad (3)$$

$$(4)$$

where  $x$  is the interaction depth,  $\lambda_e$ ,  $\lambda_h$  are the mean free paths of the electron and hole, respectively.

Similarly for the third case, the equation of the induced charges is written as follows

$$Q(x) = e \sum_{i=1}^{\frac{E}{\varepsilon}} \left( \frac{P_e + P_h}{d} \right) \quad (5)$$

$$\lambda^* = \lambda(-\ln \gamma) \quad (6)$$

$\gamma$  is a random number between 0 and 1.

$$\text{If } \lambda_e^* > d - x \text{ and } \lambda_h^* > x \longrightarrow P_e = d - x, P_h = x,$$

$$\text{If } \lambda_e^* > d - x \text{ and } \lambda_h^* < x \longrightarrow P_e = d - x, P_h = \lambda_h^*,$$

$$\text{If } \lambda_e^* < d - x \text{ and } \lambda_h^* > x \longrightarrow P_e = \lambda_e^*, P_h = x,$$

$$\text{If } \lambda_e^* < d - x \text{ and } \lambda_h^* < x \longrightarrow P_e = \lambda_e^*, P_h = \lambda_h^*, \quad (7)$$

The pulse height spectra from these calculations were then compared with the measured pulse height spectra. Fig.1 is an example of the 40 keV photon beams. It can be seen from this figure that the third case gives the best fit to the 40 keV measured spectrum. After comparison for all photons, the third case of an exponential distribution of the drifting distance of the carrier was adopted.

In the calculation of the angular dependence of the detector efficiency, the monodirectional parallel beam was assumed to be incident to the surface of CZT at the incident angle  $\theta$ . In the slant incidence, the following correction was applied to the sensitive surface of the detector

$$S = S_t \sin \theta + S_l \cos \theta \quad (8)$$

where  $S$  is the total surface of the CZT detector faced to the monodirectional parallel beam,  $S_t$  is the front surface and  $S_l$  is the lateral surface of the detector.

## 4 Results and Discussions

### 4.1 Pulse height spectra

The output pulse height spectra were measured with the multi-channel analyzer. The noise level of the detector system was about 6 keV. Figures 1 to 4 show the comparison of measured and calculated pulse height spectra of 40 keV X-ray beams,  $^{57}\text{Co}$  (14.4, 122.1 and 136.5 keV),  $^{137}\text{Cs}$  (661.7 keV) and  $^{88}\text{Y}$  (898 and 1836 keV) sources in counts per unit fluence incident to the CZT detector. In order to compare with the measured spectra, the energy deposited in the detector calculated by the EGS was smeared out using a Gaussian distribution having an energy resolution determined from the measured photopeak spectra.

For 40 keV X-ray source, there can be seen a single sharp photopeak in Fig.1 (Case 3). The full-width at half-maximum (FWHM) of the 40 keV photopeaks is 4.3 keV. The measured pulse height distribution of the 40 keV X-ray presents two escape peaks at 10 keV from  $\text{K}_\alpha$  X-ray of Te and at 14 keV from  $\text{K}_\alpha$  X-ray of Cd in Fig.1. The calculated spectra for these three cases show good agreement with the measured spectra above the noise level of 6 keV in absolute values, although the calculation does not consider the two escape peaks of 10 and 14 keV for 40 keV X-rays.

For  $^{57}\text{Co}$ , the pulse height spectra for the above three photon energies were calculated separately and summed up considering their branching ratios. The photopeaks of 122 and 136 keV are much

broader than that of 14 keV. This is because the charge collection efficiency in the detector decreases for low applied voltage of only +24V and also the energy loss through the Compton scattering increases with increase of photon energy.

The energy responses of two photon energies of 1836 keV and 898 keV for  $^{88}\text{Y}$ , were calculated separately and added taking into account the branching ratio of each energy. For higher energy photons from  $^{137}\text{Cs}$  and  $^{88}\text{Y}$ , the photopeak cannot clearly be seen because of energy loss dominated by Compton scattering and a small fraction of energy deposition in 2 mm thick CZT detector. Then, the measured spectra have monotonically decreasing shapes. The agreement between the measured and calculated pulse height spectra for these three photon sources is very good.

In this study, we used low bias voltage of +24V sacrificing better energy resolution obtained with higher bias voltage. Since our aim is to develop a gamma ray monitor of high sensitivity in this work, the low bias voltage is preferred for reasons of portability. Generally speaking, the agreement between the measured and the calculated pulse height spectra is good in absolute values over the wide energy range of 10 keV (not shown here) up to 1836 keV.

## 4.2 Energy dependence of the detection efficiency

To get the detection efficiency, the measured and calculated pulse height spectra were first summed up above the cut-off energy fixed at 6 keV. But for  $^{241}\text{Am}$  the subsidiary peaks from K X-rays and the 26.4 keV gamma ray were not considered and the two peaks of 14 and 136 keV gamma rays of  $^{57}\text{Co}$  were also excluded from the measured results in the efficiency estimation. The counts thus-obtained were normalized to unit photon fluence incident on the detector to get counts per  $\text{cm}^2$ . This value was converted to counts per unit equivalent dose in mSv by using the fluence-to-equivalent dose conversion factor ( $\text{mSv per cm}^{-2}$ ) for the A-P (anterior-posterior) geometry given by ICRP Publ.74[8]. We finally obtained the detection efficiency in cps (count per second) per mSv/h from 10 keV to 1836 keV as shown in Fig. 5.

For  $^{60}\text{Co}$  gamma rays the measured result is 20% higher than the calculated result, while for other photon energies the agreement between experiment and calculation is quite good within 3%. The efficiency is high for 10 keV and rather flat from 20 keV to 120 keV, and rapidly decreases with energy. The high efficiency at 10 keV is due to the small value of the fluence-to-equivalent dose conversion factor.

## 4.3 Angular dependence of the detection efficiency

The angular dependence of the detection efficiency with  $^{241}\text{Am}$ ,  $^{57}\text{Co}$ ,  $^{137}\text{Cs}$ ,  $^{60}\text{Co}$  and  $^{88}\text{Y}$  photon sources were also studied and we found a good agreement between experimental and calculated results except for  $^{60}\text{Co}$  with a standard deviation of about 20%. The angular dependence of the efficiency is almost constant for  $^{137}\text{Cs}$ ,  $^{60}\text{Co}$  and  $^{88}\text{Y}$  in the directions of 0 to  $90^\circ$ , but for lower energy photons of  $^{241}\text{Am}$  and  $^{57}\text{Co}$ , the efficiency decreases beyond  $60^\circ$  because of the self-absorption through the thicker layer for slant incidence. These results revealed that this CZT detector has an almost isotropic efficiency within  $60^\circ$ .

## 4.4 Effect of various filters

Figure 6 shows the variation of the efficiencies for 10, 20 and 40 keV X-rays with various thicknesses (mm) of Al filter. Solid lines are the measured results and the dotted lines the calculated results. The cut-off energy was also fixed at 6 keV. The variation of the efficiency with Al filter thicknesses is significant at 10 keV but is negligible at 40 keV. The agreement between measurement and calculation is good.

## 5 Configuration of Flat Energy Response

By utilizing the results obtained, we tried to obtain flat energy response to effective dose of the CZT semiconductor detector in the energy range of 10 keV to 7 MeV. This is an indispensable characteristic for use as a gamma-ray monitor. As very good agreement between experiment and calculation was obtained, we extend to obtain flat energy response for higher energies up to 7 MeV by calculation. Three parameters were considered for this realization: filters, cut-off energy and detector size.

The energy responses of the detector with different kinds of filter materials such as Al, Cu, Cd, Fe and Pb with various thicknesses were calculated in the energy range from 10 keV to 7 MeV. Low energy photons are very sensitive to filter material while high energy photons are almost insensitive to any kind of filters. We therefore found that it is rather difficult to get a flat response only using filters.

At the same time, we varied the cut-off energy of the pulse height spectra from 6 to 1500 keV. For low energy below 100 keV, a flat energy response of the detection efficiency can be obtained with a cut-off energy around 6 keV but for higher energy, a cut-off energy higher than hundreds of keV is necessary.

By combing these above-mentioned results parametrically, we tried to get the flat energy dependence of the detection efficiency to equivalent dose in units of cps per mSv/h within  $\pm 30\%$  and  $\pm 10\%$  differences over a wide energy region of 10 keV to 7 MeV. After many parametric surveys on filters, cut-off energies and detector sizes, we finally optimized to achieve the flat detection efficiency to equivalent dose,  $\varepsilon$ , by using two sizes of the CZT detectors;  $3 \times 3 \text{ mm}^2$  by 2 mm thick CZT, and  $10 \times 10 \text{ mm}^2$  by 2mm thick CZT; as follows,

$$\varepsilon(\text{cps per } \mu\text{Sv/h}) = \sum_i a_i \varepsilon_1 + \sum_i b_i \varepsilon_2 \quad (9)$$

where  $\varepsilon_1$  and  $\varepsilon_2$  are the detection efficiencies of  $3 \times 3 \times 2 \text{ mm}^3$  and  $10 \times 10 \times 2 \text{ mm}^3$  CZT, respectively, and  $a_i$  and  $b_i$  are multiplication factors. Fig. 7 and 8 show the results obtained by the above process using Eq.(9).

## 6 Conclusion

In this study, the pulse height spectra and the detection efficiencies of the CZT detector of  $10 \times 10 \text{ mm}^2$  by 2 mm thickness are presented for 10 keV to 1.8 MeV photon energies from both experiment and calculation using EGS4 code. The agreement between the experiment and the calculation is very good in absolute values.

The variation of the detection efficiency with the cut-of energy and with various filters was also obtained by calculation in the photon energy of 10 keV to 7 MeV. By using two CZT detectors,  $10 \times 10 \text{ mm}^2$  by 2 mm thick CZT with 1.2 mm Pb filter and  $3 \times 3 \text{ mm}^2$  by 2 mm thick CZT without filter, we finally obtained the flat energy response to effective dose within  $\pm 30\%$  and  $\pm 10\%$  deviations in the photon energy 15 keV to 7 MeV by taking the weighted sum of counts integrated above a few different cut-off energies for the two CZT detectors. From these results, it is evident that it is possible to realize a gamma ray monitor of good quality having a flat energy response to equivalent dose in a wide photon energy range. Field measurements will be further needed to compare with other commercially available survey meters.

## Acknowledgement

We are grateful to Professors H. Hirayama and S. Ban, Drs. T. Kurosawa and Y. Namito for their fruitful collaboration and advices during the calculation and experiment at KEK.

## References

- [1] J. Franc, P. Haschl, E. Belas, R. Grill, P. Hledek, P. Moravec, J. Bok, “CdTe and CdZnTe crystals for room temperature gamma-ray detectors”, *Nucl. Instrum. Methods A* **434**(1999)146-151.
- [2] A. S. Zerrai, K. Cherkaoui, G. Marrakchi, G. Bremond, P. Fougères, M. Hage-Ali, J. M. Koebel, P. Siffert, “Influence of deep levels on CdZnTe nuclear detectors”, *Journal of Crystal Growth* **197**(1999)646-649.
- [3] S. E. Pfantiel, K. J. Hofstetter, T. A. DeVol, “Comparison of four types of gamma and X-ray detectors for environmental applications in the 10-450 keV energy range”, *Journal of Radioanalytical and Nuclear Chemistry* **223 1-2**(1997)89-98. for air, nitrogen at 30 keV”, *Appl. Radiat. Isot.* **44**(1993)769-772.
- [4] H. Hirayama, “Overview of the EGS4 Code System”, *KEK Internal 97-10*, High Energy Accelerator Research Organization, 1997, pp. 6-14.
- [5] H. Nishizawa, K. Ikegami, K. Takashima, T. Usami, T. Hayakawa, T. Yamamoto, “Development of Multi-layered CdTe Semiconductor Detectors”, *Ionizing Radiation Journal* **Vol.22, No.3**(1996)27-36.
- [6] Y. X. Dardenne, T. F. Wang, A. D. Lavietes, G. J. Mauger, W. D. Ruhter, S. A. Kreek, “Cadmium Zinc Telluride Spectral modeling”, *Nucl. Instrum. Methods A* **422**(1999)159-163.
- [7] Y. Eisen, A. Shor, “CdTe and CdZnTe materials for room temperature X-ray and gamma ray detectors”, *Journal of Crystal Growth* **184/185**(1998)1302-1312.
- [8] International Commission on Radiological Protection, “ Conversion Coefficients for use in Radiological Protection against External Radiation”, *ICRP Publication 74, Annals of the ICRP* **Vol.26/3**, 1995.

Table 1. Physical characteristics of the CZT detector

Size	10 x 10 x 2 mm <sup>3</sup>
Density	5.86 g·cm <sup>-3</sup>
Resistivity	3 x 10 <sup>10</sup> Ωcm
Band gap	1.56 eV
Mobility and lifetime product	3x10 <sup>-3</sup> cm <sup>2</sup> ·V <sup>-1</sup> for electron and 2x10 <sup>-5</sup> cm <sup>2</sup> V <sup>-1</sup> for hole
Depletion layer	2 mm

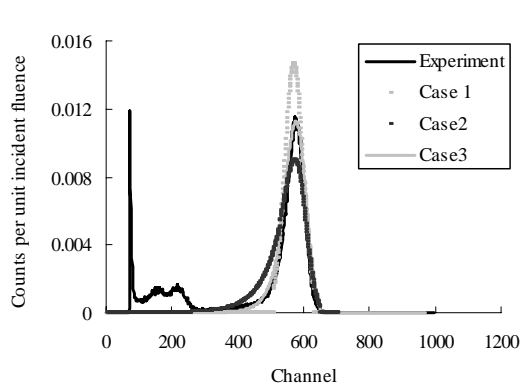


Fig.1 Comparison of measured pulse height spectra for 40 keV X-rays with the calculated spectra for three models of charge collection. Case 1: Energy absorption only; case 2: Constant drift distance of carriers; case 3: The drift distance of carriers has an exponential distribution

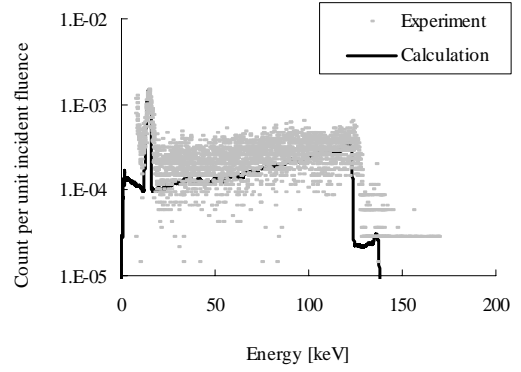


Fig.2 Pulse height spectra of <sup>57</sup>Co photon source

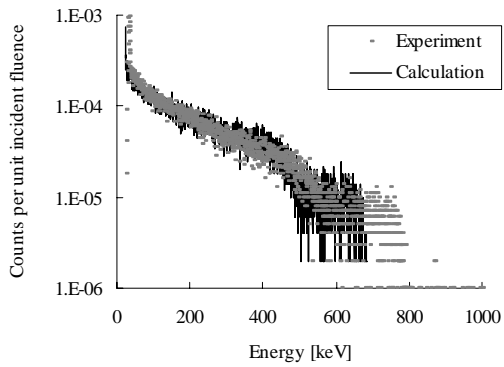


Fig.3 Pulse height spectra of <sup>137</sup>Cs photon source

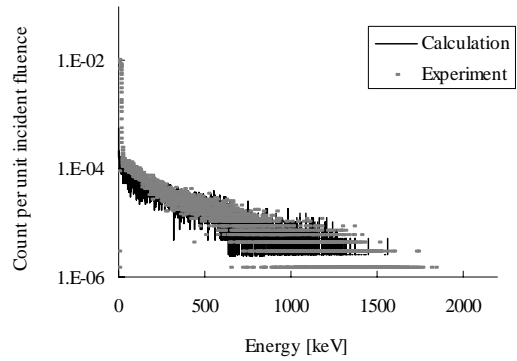


Fig.4 Pulse height spectra of <sup>88</sup>Y photon source

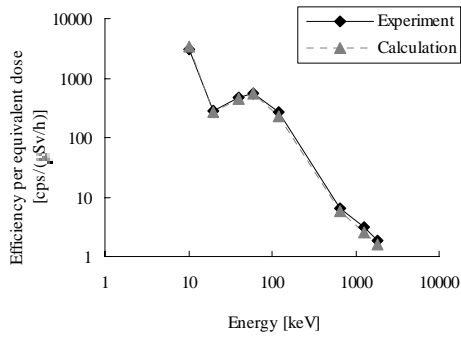


Fig.5 Measured and calculated detection efficiencies of the CdZnTe semiconductor detector as a function of photon energy

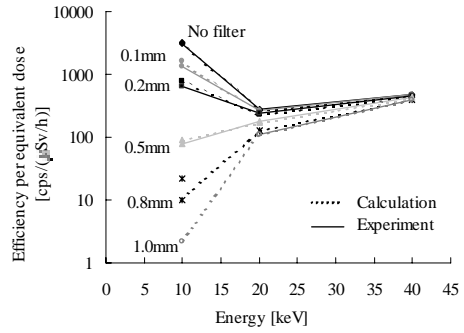


Fig.6 Variation of the detection efficiency with aluminum filter for 10 to 40 keV photons

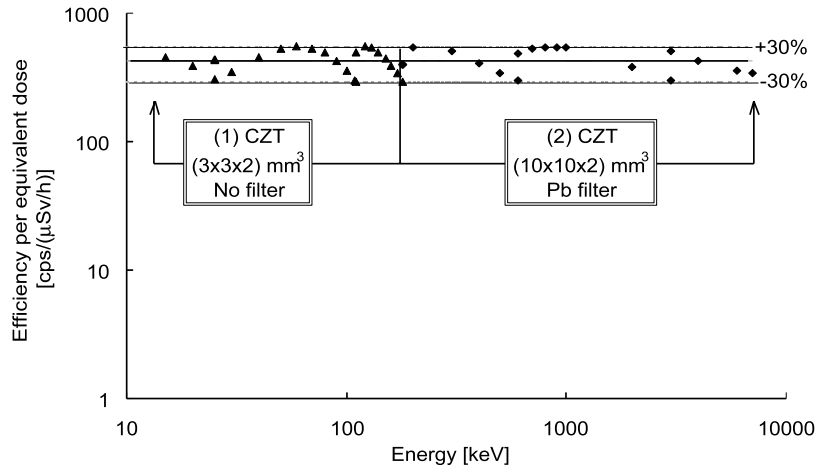


Fig.7 Energy dependence of detection efficiency to effective dose within 30% difference.

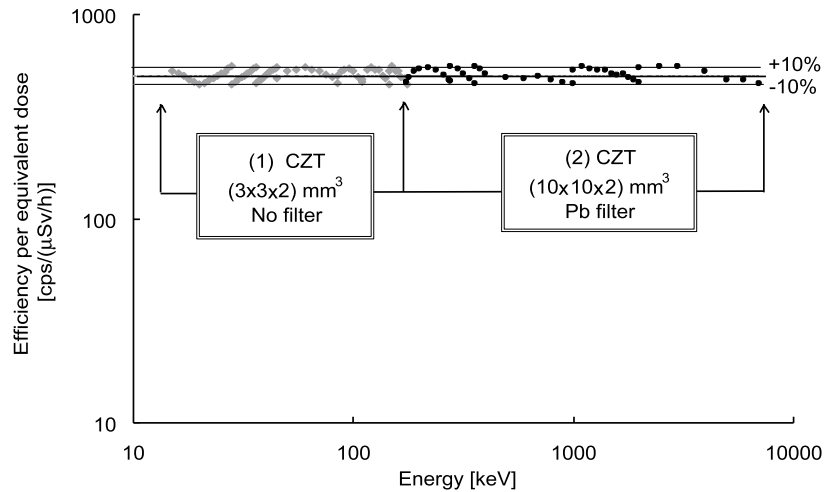


Fig.8 Energy dependence of detection efficiency to effective dose within 10% difference.